applied sciences

MDPI

Article

Establishment of the Controlled Low-Strength Desulfurization Slag Prediction Model for Compressive Strength and Surface Resistivity

Chang-Chi Hung [1], Chien-Chih Wang [2] and Her-Yung Wang [3,*]

[1] School of Architecture and Civil Engineering, Huizhou University, Huizhou 516007, China; a0266@hzu.edu.cn
[2] Department of Civil Engineering and Geomatics, Cheng Shiu University, Kaohsiung City 83347, Taiwan; ccw@gcloud.csu.edu.tw
[3] Department of Civil Engineering, National Kaohsiung University of Sciences and Technology, Kaohsiung City 80778, Taiwan
* Correspondence: wangho@nkust.edu.tw; Tel.: +886-7-381-4526-15237

Received: 24 June 2020; Accepted: 13 August 2020; Published: 15 August 2020

Abstract: In this study, the desulfurization slag used the volume method to replace fine natural aggregates in controllable low-strength materials (CLSM); the desulfurization slag content (DS) and curing time (t) were used as variables to test the compressive strength and surface resistivity of CLSM and simulated a prediction model on the results. The test results showed during that the compressive strength on the 28th day, the average desulfurization slag replacement amount increased by 10%, and the compressive strength decreased by 0.9 MPa. The surface resistivity increases with age, and each ratio increases from seven days to 28 days, and the surface resistivity value increases from 9.3% to 20.6%. After that, a hyperbolic function and exponential function with multiple variables were used to establish a simulation model of the effects of the DS content and curing time on the compressive strength and surface resistivity of CLSM. Compared with the test results, the statistical analysis shows that the average absolute percentage error (MAPE) of the compressive strength is 9.17%, and the surface resistivity is 10.67%. From the results, the predictive analysis model developed in this paper provides good predictive results in terms of compressive strength and surface resistivity.

Keywords: controlled low-strength materials; desulfurization slag; compressive strength; surface resistivity

1. Introduction

Countries all over the world are eager to research the reuse of industrial waste, turning industrial waste into reusable resources and, at the same time, moving towards the goal of carbon reduction. This research follows the principles of waste reduction, resource reuse, and a safe economy. Therefore, the application of silicic acid slag to controllable low-strength materials is discussed to effectively control the generation of waste, properly handle it, and make up for the shortage of sand. Global steel production peaked in 2014, reaching 1.6 billion tons, of which Asian production accounted for 60% of the total production; China's production accounted for 800 million tons of total production. Japan, India, the United States, South Korea, and Russia are also the largest producers. The global output of 1.6 billion tons of steel produces about 250 million tons of slag. Now, the annual output of desulfurized slag from the Taiwan Iron and Steel Company is about 300,000 tons [1].

Desulfurization slag (DS) is the solid waste generated in the molten iron desulfurization process by the desulfurization agent in the blast furnace. Therefore, it is a product produced during the high-temperature melting process. Its physical properties are tolerant to high temperatures and are

less influenced by climate change. Its chemical properties are very stable and safe, and the mobility of heavy metals is low. It can also partially replace limestone or be used as a backfill material for soil and stone during the cement clinker firing process [1]. The molten iron in blast furnace steel contains sulfur; it is hot. After the torpedo car, the sulfur is removed by a desulfurizing agent, and the obtained slag body is discharged into the torpedo car and then slowly cooled to a fine granular shape, and because of the high content of SiO_2 in the components thereof, it is also called the sulfur residue. Since the desulfurized slag still contains a part of the slag, after subsequent processing, such as magnetic partition, crushing, and smashing, the slag can be recovered, which improves the purity and utilization value of the desulfurized slag [2]. In recent years, some studies have been carried out to replace part of the natural coarse aggregate and fine aggregate with desulfurized slag in the design of concrete mix ratio and applied to cement mortar [1–7]. From the study of Kuo and Shu (2014) [2], it was found that desulfurized slag can be used to replace the natural sand in the cement mortar mixture, and it was pointed out that, if the mortar solidified at a high temperature and the desulfurized slag replacement rate increased, the mortar volumetric expansion tended to increase, and the rate of volumetric expansion increased. Additionally, as the desulfurization slag replacement rate increases, the compressive strength tends to decrease [5–8].

In recent years, countries and regions around the world, such as the United States, Canada, Europe, Israel, Japan, and other countries, have developed a highly mobile to improve the quality of backfill engineering, reduce costs, reduce manpower, and reduce the impact of traffic. Controlled low-strength materials (CLSM) has been widely used in foundations, roads, and pipeline-backfilling projects. It is a new type of cementitious material that replaces traditional backfilling materials and can be applied to solve the problem of pipeline excavation. The lack of artificial compaction leads to the loss of road surface subsidence, cracks, and road surface flaking and reduces the noise caused by the use of a large number of tamping workers and construction [9,10]. Additionally, CLSM has no special restrictions on the requirements of aggregates. Recycled aggregates such as abandoned masonry, concrete, and cast sand are also ideal materials for CLSM. The water-binder ratio of CLSM is between 1 and 1.5, which is much higher than the water-binder ratio of 0.4–0.55 for general concrete. The raw materials used in CLSM and general concrete are not significantly different. They are also composed of coarse aggregate, fine aggregate, water, cement, and concrete. The coarse aggregate of CLSM is about 200–400 kg/m^3. The amount of inter- and fine-shaped aggregates is between 1280 and 1480 kg/m^3, which is between 700–1100 kg/m^3 of general concrete coarse aggregate and 700–1000 kg/m^3 of fine aggregate [11–13]. According to the American Concrete Association (ACI) definition, all flowable backfill, low-shrinkage controllable low-strength backfill, flowable slurry, plastic clay cementitious material, and K-Krete can be generalized CLSM [11].

Based on the early strength, many studies have been conducted to predict and analyze the compressive strength of concrete or cement mortar at 28 days or other days [14–18]. The results of the study show that, if some aggregate substitutes (including fly ash, slag, and waste glass) are used, the compressive strength will increase with the increase in curing time, but this increase will become stable. Previous researchers used the math function to calculate the relationship between the surface resistivity of concrete and curing age and proposed a math relationship between the compressive strength and resistivity [19–22]. However, few people have proposed a prediction model for the compressive strength and surface resistance of CLSM containing desulfurization slag.

This study shows that when the desulfurization slag replacement content is applied to CLSMs, it will influence the compressive strength and resistivity and, also, establish a good prediction model, which will serve as a reference for subsequent research and engineering applications. Additionally, this study attempts to establish the prediction results of the compressive strength and surface resistivity of CLSMs using the relevant mathematical functions. When the prediction mode is established, to provide a reference design, reduce the mixing workforce, test the cost of materials, and save time, the results of the preliminary test can also be applied to evaluate the material strength and durability in the later stages. Wang et al. [15,23] have studied the effects of compressive strength, flexural

strength, ultrasonic wave velocity, waste glass content, water-binder ratio, and curing age for a series of matching test results of self-filling waste liquid crystal glass concrete. The relationship between the factors and, according to the test results, the hyperbolic function, the exponential function, and the power function, are used to perform a nonlinear multivariate regression analysis, and the prediction can be reasonably evaluated. Therefore, this paper will analyze and verify the compressive strength and resistivity of controlled low-strength desulfurization slag materials according to the prediction model proposed by the author and others for waste liquid crystal glass concrete to evaluate whether the analysis mode is applicable for further research. It is intended to be suitable for the predictive model of controlled low-strength desulfurization slag materials. Similarly, the starting point of waste reprocessing and sustainable development, including the addition of desulfurized slag and other raw material alternatives of CLSMs, constitutes a good research topic of the study.

2. Test Program Experimental Materials and Mixtures

2.1. Test Materials

1. Cement: Use Type I Portland cement produced by Taiwan Cement Corporation, Taiwan, China Ltd.; Its chemical components are listed in Table 1. Its characteristics correspond to those of Type I Portland cement specified in ASTM C150.
2. Fly ash (FA): Use Class F fly ash produced by Taiwan Power Xing-Da Firepower Plant, Taiwan, China. Its properties are chosen in compliance with ASTM C618 specifications. Table 2 shows the chemical ingredient of fly ash.
3. Mixing water: Corresponds to ASTM C94 for concrete mixing water.
4. Natural Aggregate (NA): The natural sand used in this study; the particle size distribution curve obtained after the sieve analysis test conforms to ASTM C33 specifications, and then, the basic properties such as specific gravity and water absorption rate are tested separately. See Table 2.
5. Desulfurization slag (DS): Desulphurization slag was from Taiwan Ti-Sa Chemical Industrial Corp, Taiwan, China; It is the residue after the ground particle blast furnace slag is refined by the magnetic separation method. The slag is a fine aggregate passed through a # 4 (4.75-mm) sieve. The fineness is close to the particle size of natural aggregates. Table 1 shows the chemical and physical properties of the desulfurization slag.

Table 1. The chemical properties of the materials.

Properties	Chemical Properties (%)		
	Cement	Fly Ash	Desulfurization Slag (DS)
SiO_2	20.18	50.79	9.92
Al_2O_3	4.95	24.97	4.22
Fe_2O_3	2.82	7.87	8.22
CaO	64.40	5.68	69.02
MgO	2.32	1.72	2.32
SO_3	2.45	0.30	4.30
Alkalis	0.48	-	-
K_2O	-	-	0.06
Na_2O	-	-	0.14
P_2O_5	-	-	0.17
MnO	-	-	0.60
Cr_2O_3	-	-	0.08
LOI	2.39	3.10	-
f-CaO	-	-	0.95

Table 2. The physical properties of the materials.

Materials	Specific Gravity	Unit Weight (kg/m^3)	Water Absorption (%)	Fineness Modulus
Coarse Aggregate	2.640	1582	0.9	-
Fine Aggregate	2.631	1873	1.6	3.05
Desulfurization Slag	2.380	1011	38.0	2.80

2.2. Test Variables and Method

In order to find the best replacement amount and the best proportion of adding desulfurization slag materials to CLSM, in this study, the DS passing through the # 4 (4.75-mm) sieve was used to replace the fine natural aggregate by the volume method (0%, 10%, 20%, 30%, 40%, and 50%) mixed into a CLSM. Following ASTM C192, after several different proportions of trial mixing, the water-binder ratio (w/b) of the CLSM control group is set to 1.5, the ratio of the cement to aggregate is 1:9, the amount of fly ash added is 10% of the total binder (20kg/m^3) to increase its fluidity, the fixed amount of coarse aggregate is 400 kg/m^3, and the CLSM special quick-setting agent, which accounts for 2% of the binder, is added to shorten the initial setting time and speed up the road-opening time. The slump is set to 40 cm or more. The mixture proportions of the CLSM is shown in Table 3. The CLSM samples were cast and cured. Take them out after 24 h and set them in saturated lime water at room temperature (23–25 °C) to solidify. In this study, six kinds of proportions were tested at the ages of 1, 3, 7, 28, 56, and 91 days. After testing 3 samples in each case, the test results were averaged to obtain its compressive strength and surface resistivity. Develop the obtained test results into a mathematical prediction model for future use. The compressive strength test was conducted in accordance with ASTM C39 specifications, and a cylindrical specimen of ψ10 cm × 20 cm was made and cured at room temperature. During a surface resistance test, measured in accordance with ASTM C876 specifications, the instrument is calibrated to zero before the test, and the test specimen is in a saturated state in the surface area during the test. These measurements are carried out at day 1, day 3, day 7, day 28, day 56, and day 91.

Table 3. The controllable low-strength material (CLSM) mixing proportions (unit: kg/m^3). w/b: water-binder ratio.

	DS (%)	CLSM Special Accelerator	Cement	Fly Ash	Desulfurization Slag	Sand	Coarse Aggregate	Water	w/b
CLSM	0	3.8	170	20	0	1312	400	285	1.5
	10	3.8	170	20	119	1181	400	285	1.5
	20	3.8	170	20	237	1050	400	285	1.5
	30	3.8	170	20	356	918	400	285	1.5
	40	3.8	170	20	476	788	400	285	1.5
	50	3.8	170	20	595	658	400	285	1.5

2.3. Test Equipment

1. Compressive strength-testing machine.

The test equipment is a 30-ton concrete compression machine, as shown in Figure 1a. The axis of the test specimen must coincide with the center axis of the spherical seat.

2. Four-pole resistance-measuring instrument.

The concrete resistivity-measuring instrument used in this test is a four-pole resistance-measuring instrument produced by PROCEQ, Schwerzenbach, Switzerland. The surface resistivity of the concrete is measured after the four-pole probe is in contact with the concrete, and the current is set at 180 μA, frequency 72 Hz, impedance 10 MΩ, measuring range 0–99 kΩ-cm, and accuracy ±1 kΩ-cm. The electrode spacing of the four-pole resistance meter used is fixed at 5 cm, and the tip of the sponge

between the electrodes must be moistened with clean water before use to avoid the inability to conduct electricity and affect the measured resistivity. The larger the surface resistance, the smaller the corrosion current. The two have a good Ohm's law (V = IR) relationship, where V is the voltage measured across the conductor in units of volts, I is the current through the conductor in units of amperes, and R is the resistance of the conductor in units of ohms. The concrete resistance represents the durability index of the concrete density and impermeability and is a necessary measurement for the durability of high-performance concrete. It is generally stipulated that the resistance of concrete over 56 days must be greater than 20 kΩ-cm, which is considered to be excellent durable concrete, as shown in Figure 1b.

Figure 1. Test equipment. (**a**) Compressive strength-testing machine. (**b**) Four-pole resistance-measuring instrument.

3. Test Results and Analysis

3.1. Compressive Strength

Compressive strength is often regarded as an important indicator of CLSM quality. Figures 2 and 3 present the relationship of the desulfurization slag content (DS) and curing time (*t*) on the compressive strength of a CLSM. Figure 2 shows the compressive strength of the CLSM, indicating that the DS replacement is between 0% and 50%, the compressive strength at the age of one day is 0.2–1.3 MPa, and the compressive strength value of the test group with the DS substitution amount of 10% to 50% is lower than the control group's compressive strength value between 0.9 MPa and 2 MPa. The seven-day compressive strength reduction is between 2.0 MPa and 5.5 MPa; the 28-day compressive strength reduction is between 2.7 MPa and 7.2 MPa. The compressive strength of the CLSM increases with age. If the curing age is from seven days to 28 days, the percentage of the compressive strength of each DS replacement ratio increases by 21.1–85.7%. The 28-day compressive strength of all test specimens did not exceed 9 MPa, which was in-line with the majority of the CLSM regulations in Taiwan; the growth of the compressive strength after 28 days of age was relatively flat, with each substitution group increasing by 5.3% to 10%; if the maximum substitution amount was at 50%, there was no growth in the compressive strength from 56 to 91 days of age.

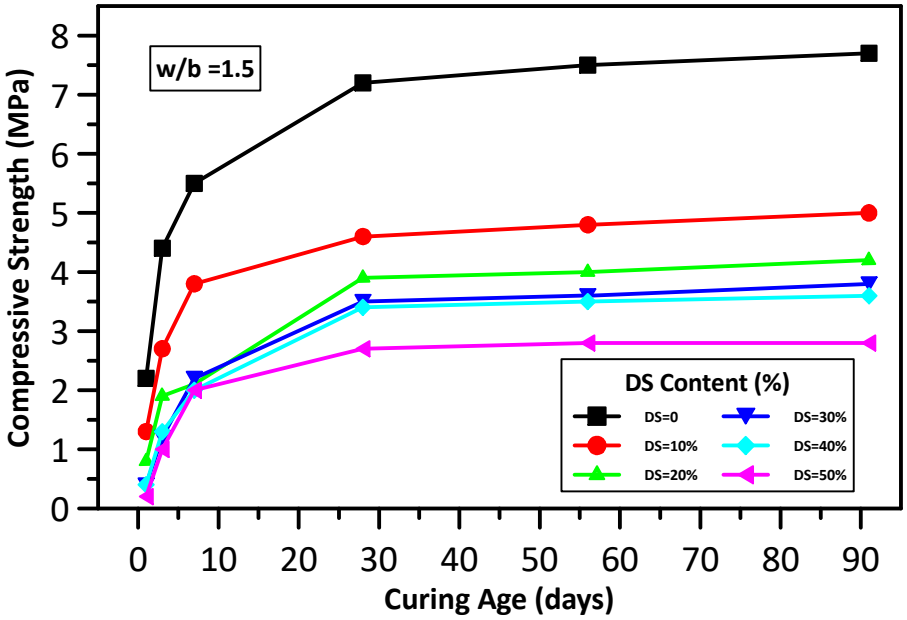

Figure 2. The relationship between the curing age and compressive strength of the controllable low-strength materials (CLSM). DS: desulfurization slag and w/b: water-binder ratio.

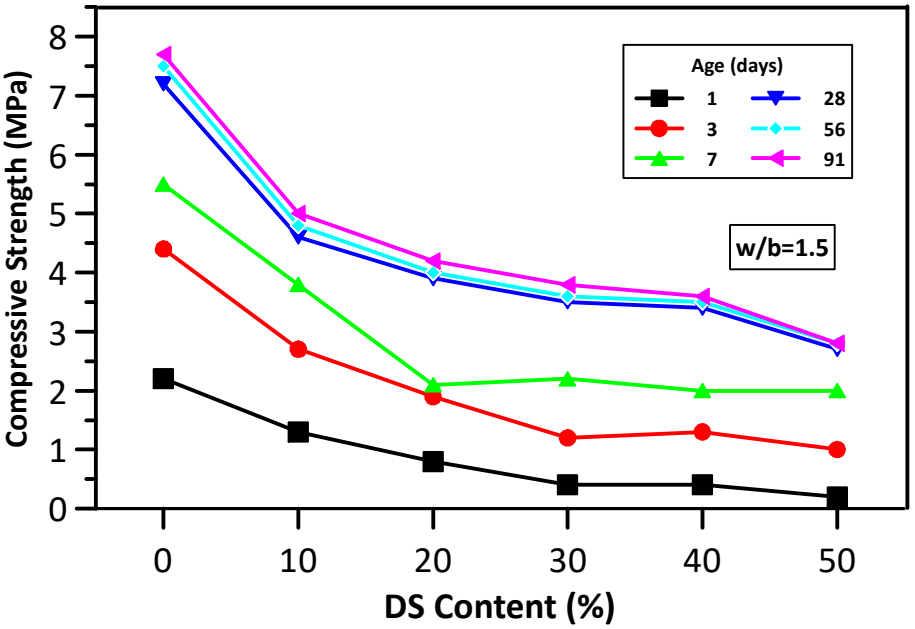

Figure 3. The relationship between the DS content and compressive strength of the CLSM.

Figure 3 shows the compressive strength development of the CLSM. At 28 days of age, the average amount of the DS replacement is increased by 10%, the compressive strength is reduced by 0.9 MPa, and the age is 28 days to 91 days. The compressive strength of each group of DS is not much different from that of the control group, and the strength reduction range is between 2.6 MPa and 4.9 MPa (36.1–63.6%). The test results show that the compressive strength increases with the increasing curing age but decreases as the DS replacement increases. When the replacement ratio of the DS is less than 20%, the compressive strength decreases rapidly with the replacement of the DS. However, when the replacement ratio of DS is between 20% and 50%, the reduction in the compressive strength value does not change much at any curing age.

It can be seen from the above that the compressive strength of the CLSM is inversely related to the substitution amount of industrial by-product DS. The more the substitution amount, the lower the compressive strength. The possible reason is that the CLSM is a high water-binder ratio material, although it improves workability. Relatively, the compressive strength is also reduced, and the particle size of the desulfurized slag is smaller than that of the fine aggregate, which is also a cause of low strength, which causes the bond formed during the coagulation to be weak and, therefore, cannot provide strength.

3.2. Surface Resistivity

Figures 4 and 5 present the test relationship of the desulfurization slag content (DS) and curing time (t) on the surface resistivity of the CLSM. The most influential factor affecting the surface resistivity is the compactness of the internal structure of the test piece. When the internal structure has fewer pores, the denser the test piece, the higher the relative resistivity and the better the durability. As shown in Figure 4, the surface resistivity increases with the increase in age. The surface resistivity increases from 9.3% to 20.6% when the curing age is from seven days to 28 days in each DS replacement ratio. It grew by 17.6–41.2% from 28 days to 56 days and grew by 17.6–39.2% from 56 days to 91 days. Compared with the surface resistivity development of the 28-day value, it is most significant at the age of 28 to 56 days. The possible reason is that the hydration of the CLSM is completed at a late age, which increases the percentage of the resistivity value growth.

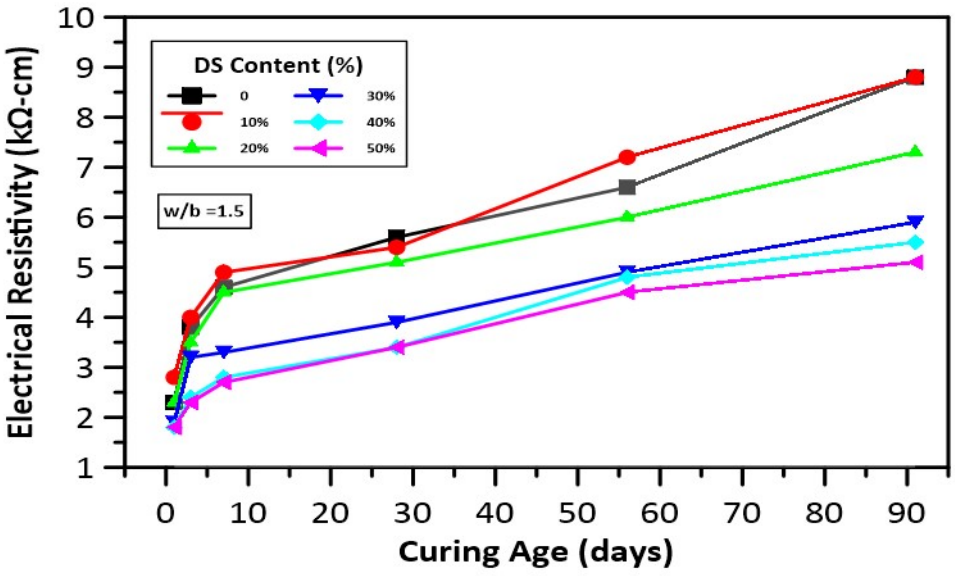

Figure 4. The relationship between the curing age and surface resistivity of the CLSM.

As shown in Figure 5, the surface resistivity of the 10% DS-replaced fine aggregate was slightly lower than the control group by 0.2 kΩ-cm at 28 days of curing age, and the resistivity development at other ages can be higher than the control group by 5.3–21.7%. The surface resistivity of the DS replacement ratio of 20% is similar to the control group at the early curing ages of one, three, and seven days, and the difference is within 0.3 kΩ-cm. After 28 days of age, the resistivity is lower than 0.5–1.5 kΩ-cm compared with the control group; after the replacement ratio is greater than 30%, the surface resistivity decreases with the increase of the replacement ratio, and it is lower 28.3–41.3% than the control group at the curing age of seven days, where the surface resistivity decreases by 30.4–39.3% at the curing age of 28 days, and the difference is 33–42% at the curing age of 91 days.

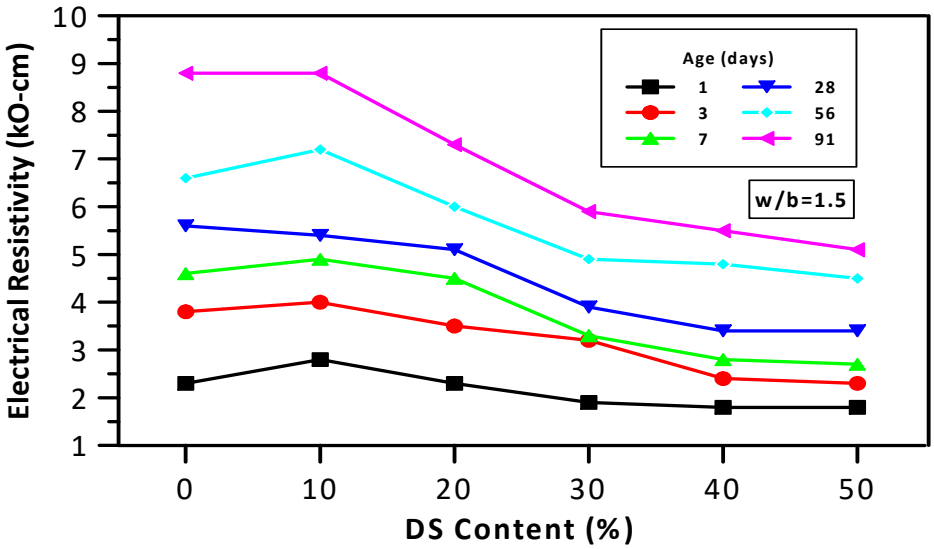

Figure 5. The relationship between the DS content and surface resistivity of the CLSM.

The reason is that the increase in the amount of substitution causes the moisture content in the test specimen to increase, and the compactness of the test specimen is relatively lowered, which is relatively affected by the development of the durability. The resistivity of the control group and the 10% to 20% substitution group and the 30% to 50% substitution group can be increased to more than 5 kΩ-cm at 28 days and 91 days as compared with the general concrete age of 56 days. The resistivity of the control group and the 10% to 20% replacement group and the 30% to 50% replacement group can be increased to more than 5 kΩ-cm at the age of 28 days to 91 days. However, compared with the 56-day curing age of ordinary concrete, the required surface resistivity is 20 kΩ-cm, and the surface resistivity of CLSMs is still much lower, due to the high water-binder ratio and the replacement of DS of the CLSMs that do not need to be compacted, and results in more pores in the hydration process. This affects the development of durability indirectly.

3.3. Regression of the Compressive Strength and Surface Resistivity

Figures 6 and 7 show the linear and logarithmic function regressions of the compressive strength and surface resistivity. With the increase of the replacement, the regression line gradually smooths, indicating that the compressive strength and surface resistivity both increase at a slow rate. As a result of the above, Figures 6 and 7 mainly hope to study the relationship between the mechanical properties (compressive strength) and durability (surface resistance) of the samples through statistical methods, such as confidence intervals. We tried to obtain satisfactory results through linear or nonlinear regression analyses, but the results were not good. R^2 is the coefficient of determination, it is the proportion of the variance in the dependent variable that is predictable from the independent variable(s). The coefficients R^2 greater than 0.7 show a significant relationship between the compressive strength and surface resistivity, but the regression results in Figures 6 and 7 show that their coefficients R^2 are less than 0.7, so it is necessary to develop other function models to predict the relationship between the compressive strength and surface resistivity.

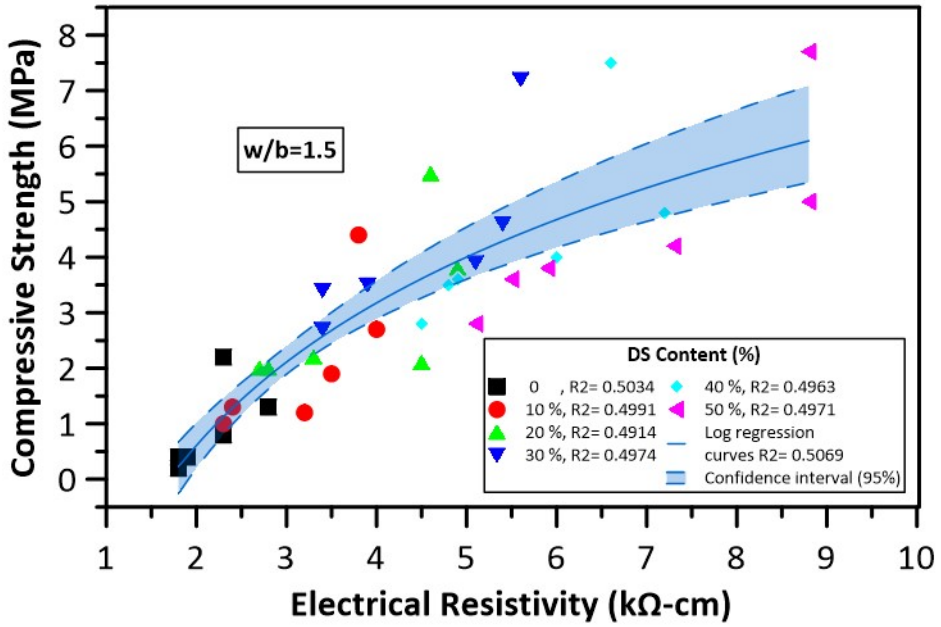

Figure 6. Logarithmic regression relationship between the surface resistivity and compressive strength with various DS ratios of the CLSM.

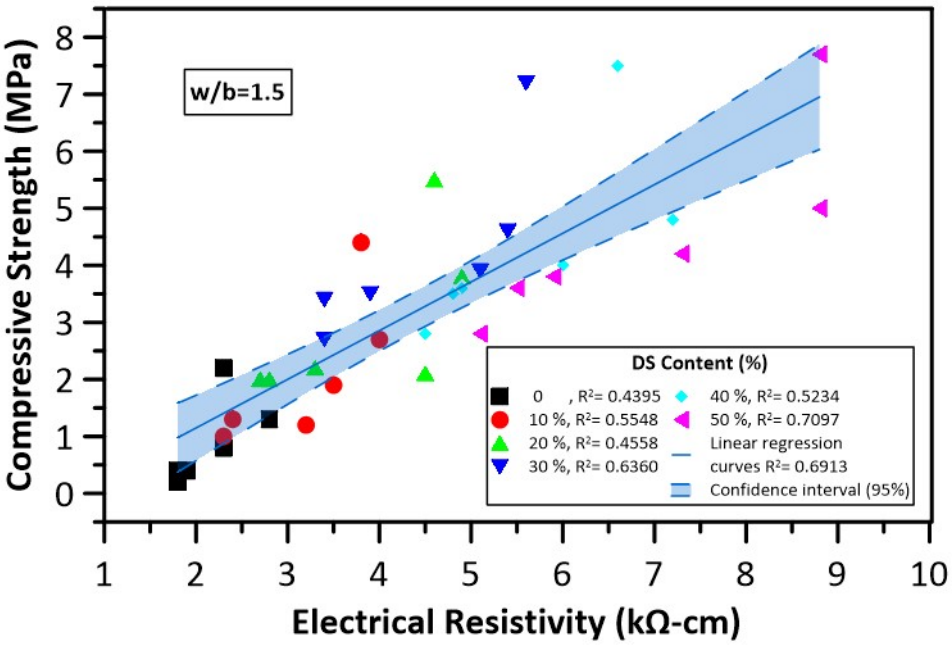

Figure 7. Linear regression relationship between the surface resistivity and compressive strength with various DS ratios of the CLSM.

4. The Compressive Strength and Resistivity Prediction Model of the CLSM

4.1. The Prediction Model of Compressive Strength

In the design of controlling low-strength DS, its compressive strength is essential. The 28-day compressive strength is usually regarded as the design strength. To ensure this power, we must wait for a long time—that is, 28 days [16]. Thus, if it is possible to prove a later compressive strength prediction model based on early strength, it will be very helpful for the application of the material and its subsequent evaluation. Many studies have been conducted to predict and analyze the compressive

strength of concrete or cement mortar at 28 days or other days based on early strength [14–18], but few people have raised the compressive strength prediction models of CLSMs containing desulfurized slag. Kheder et al. (2003) [17] proposed a series of models to predict the compressive strength of cement samples after a series of cement mortar test results. The prediction model can predict the compressive strength results of seven days and 28 days according to the compressive strength within 24 h. The model considers six variables, but up to 17 variables can be considered. If more variables are considered, the prediction accuracy will be higher. Kabir et al. (2012) [16] was based on the seven-day test results, and Alilou and Teshnehlab (2010) [24] established a 28-day compressive strength prediction analysis based on the three-day test results. The results of the study show that if some aggregate substitutes (including fly ash, slag, and waste glass) are added, the compressive strength will increase with the curing time, but this increase becomes stable over time. Wang et al.'s (2014 and 2017) [14,23] previous studies used a hyperbolic function to simulate the relationship between the compressive strength of liquid-crystal display (LCD) waste glass concrete and curing time.

Thus, the relationship between compressive strength and curing age were discussed in this study under the condition of a fixed water-cement ratio (w/b = 1.5) and the replacement rate of desulfurized slag instead of fine aggregate gradually changing from DS = 0% to DS = 50%. The final test results showed the same trend as past studies [14–18]. There is a nonlinear relationship between the compressive strength and the increase in curing time. The increasing trend of the compressive strength will gradually decrease with age and will tend to be horizontal. The CLSM is cured at room temperature. Under the condition of changing the desulphurization slag substitution rate (DS), the relationship between the compressive strength and curing age within 28 days can be expressed as a hyperbolic function, where $f'_{c,}$ is the compressive strength of any curing age, $f'_{c,28}$ is the compressive strength of 28 days of curing age, as shown in Figure 8.

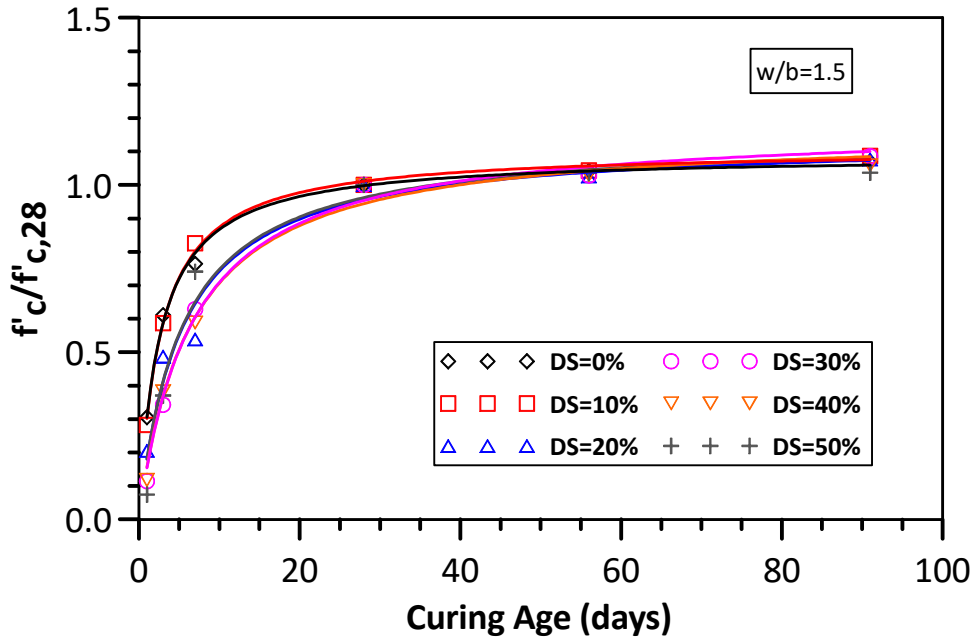

Figure 8. Hyperbolic function relationship of the compressive strength and surface resistivity with various DS contents of the CLSM.

In the prediction model of the curing age and compressive strength based on the strength test results, we will use the compressive strength at 28 days as the normalization basis, combined with the hyperbolic function, to obtain the predictive model of the controlled low-strength DS material. The compressive strength equation is shown in Equation (1), where f'_c refers to the compressive strength at any curing age, $f'_{c,28}$ refers to the compressive strength at the age of 28 days, t refers to the curing

age (1 to 91 days), DS refers to the replacement rate of desulfurization slag, a and b are the hyperbolic function coefficients of the compressive strength prediction analysis based on the DS content. R^2 is the coefficient of determination. Table 4 shows the a and b obtained when the replacement ratio of DS to the natural fine aggregate is 0%, 10%, and 20% to 50%, respectively. The coefficient value of b is normalized by compression to the strength of day 28. It will continuously predict to 56 days and 91 days. According to previous studies, the coefficient a and the coefficient b are mainly related to the curing temperature and the DS. Thus, when the curing temperature and water-binder ratio is fixed, the hyperbolic function coefficients a and b can be expressed as a function of DS, as shown in Equations (2) and (3). Figure 9 shows the simulated results of the relationship between the hyperbolic function coefficients a and b and the DS replacement rate. The value of the coefficient a is distributed in the interval of 2.3–5.7, and the relationships between the parameters a_1 and a_2 and the DS can be approximately expressed as an increasing function, as shown in Figure 9a and Equation (2). Where a_1 and a_2 are the linear regression parameters of the hyperbolic function coefficient a.

Table 4. Hyperbolic function coefficients of the compressive strength prediction analysis based on the DS content.

w/b	DS	Coefficients of Hyperbolic Function		
		a	b	R^2
1.5	0	2.3589	0.9177	0.9961
	0.1	2.4088	0.9029	0.9972
	0.2	4.6787	0.8798	0.9688
	0.3	5.6384	0.8472	0.9930
	0.4	5.5493	0.8607	0.9925
	0.5	4.6444	0.8732	0.9696

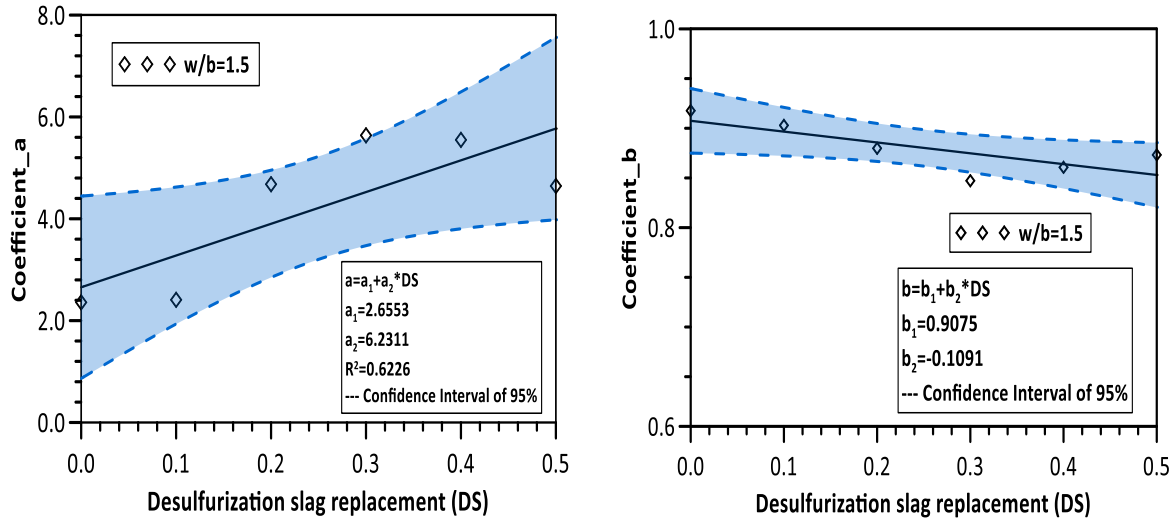

(**a**) (**b**)

Figure 9. (**a**) The relationship between the hyperbolic function coefficient a and the DS content. (**b**) The relationship between the hyperbolic function coefficient b and the DS content.

On the other hand, the value of the coefficient b is distributed between 0.84 and 0.92, and the relationships of the parameters b_1 and b_2 and the DS are approximately equal to the decreasing function, as shown in Figure 9b and Equation (3). Where b_1 and b_2 are the linear regression parameters of the hyperbolic function coefficient b. Therefore, the relationship between the CLSM's 28-day compressive strength and the DS replacement rate can be expressed as a nonlinear quadratic polynomial function. Where $f'_{c,}$ is the compressive strength of any curing age, $f'_{c,28}$ is the compressive strength of 28 days of

curing age, DS is the replacement rate of the desulfurized slag, and t is the curing age (1 to 91 days), while a_1 and a_2, and b_1 and b_2 are model parameters associated with the replacement rate of the DS. Figure 10 shows the relationship between the simulated model parameters a_1, a_2, b_1, and b_2 and the replacement rate DS.

$$\frac{f'_c}{f'_{c,28}} = \frac{t}{a + bt} \tag{1}$$

$$a = a_1 + a_2 \times DS \tag{2}$$

$$b = b_1 + b_2 \times DS \tag{3}$$

$$f'_{c,28} = x_1 + x_2 \times DS + x_3 \times DS^2 \tag{4}$$

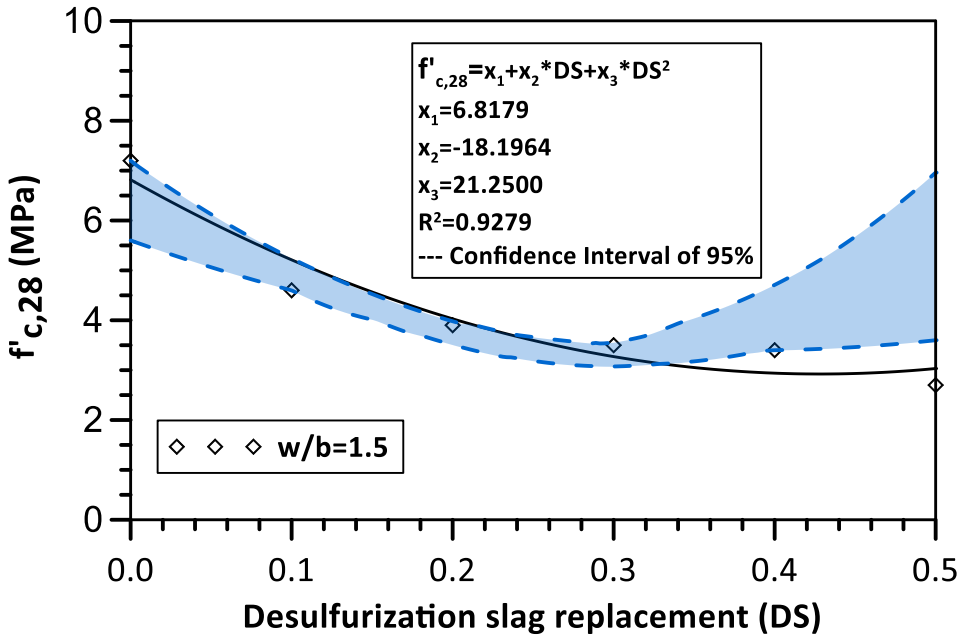

Figure 10. The relationship between the compressive strength of the CLSM, DS content, and coefficient x on the 28th day.

4.2. The Prediction Model of the Surface Resistivity

Previous researchers used the power increase function to calculate the relationship between the surface resistivity and curing age and proposed a linear relationship between the compressive strength and resistivity (Lubeck et al. (2012) [19]). Liu and Presuel-Moreno (2014) [20] used hyperbolic equations to evaluate the change of the concrete resistivity with the curing age. The results showed that the 28-day compressive strength increased nonlinearly with the increasing resistivity. However, the trend of the concrete resistivity with the increase of the specimen curing age became stable. In other studies, it was also shown that the compressive strength of the mortar at 28 days could be estimated from the resistivity of the 24-h sample, and a linear increase relationship was established (Xiaosheng et al., 2012 [21]). Additionally, in 2010, Ferreira and Jalali [22] used two methods for analysis between the surface resistivity and curing age. First, a hyperbolic equation was proposed to simulate the change in surface resistivity over time. Second, the exponential function was used to predict the relationship between the resistivity of the theoretical method model and the curing age. Wang and Chen (2010) [25] also used a hybrid design of controlled low-strength concrete using different water-binder ratios and concrete mixed with discarded LCD glass sand instead of different percentages of sand. It was found that the electrical resistivity increased with the increase of the curing age but decreased with the increase of the water-binder ratio. The resistivity increased as the

percentage of glass sand substitutes increased. Therefore, based on the characteristics of the surface resistivity, this study considers the surface resistivity of CLSMs, including variables such as the curing age t and DS replacement rate DS, to infer the predicted model of CLSM resistivity.

The results of past research indicate that the resistivity of waste glass concrete increases with the increase of waste glass (Wang and Chen, 2010 [25]). Therefore, the prediction model in this study assumes that when the same mixing ratio is used to increase the DS content, the specific resistivity of the CLSM will increase. The model is deduced in the exponential function for use in predictive models and the relationship between surface resistivity and curing age, as shown in Figure 11. Where E_r is the surface resistivity and t is curing age. The deduced mathematical model in this study will assume that, when the same water-binder ratio is used, and the ratio of the DS replacement is increased and the resistivity of the CLSM increases. Figure 11a shows the test results of the resistivity E_r and the different curing ages of the CLSMs with different DS replacement ratio DS when the water-binder ratio (w/b) is 1.5. For the same DS replacement ratio DS, the resistivity E_r exhibits a slight nonlinear increase with the curing age t. However, the nonlinear relationship is not obvious. As the content of the DS increases, the electrical resistivity also increases. Figure 11b shows that, in the semi-log scale coordinates, the relationship between the surface resistivity and curing age t has a significant nonlinear increase, and as the curing age increases, the increase becomes smooth. Therefore, the relationship between the resistivity and curing age is simulated using an exponential function equation, as shown in Equation (5). Where f_c' refers to the compressive strength at any curing age, f_{c0}' refers to the compressive strength is given by tested results, E_r is the surface resistivity at any curing age, E_{r0} is the surface resistivity is given by tested results, t refers to the curing age (1 to 91 days), DS refers to the replacement rate of desulfurization slag, Where a_e and b_e are exponential function coefficients of the surface resistivity prediction model based on the DS content. Among them, the coefficients a_e and b_e are shown in Table 5 and the relationship with curing age t has a significant nonlinear increase. When Equation (5) is passed back to normal scale coordinates, it can be rewritten as Equation (6):

$$y = log_{10}E_r = f(t) = \frac{t}{a_e + b_e t} \tag{5}$$

$$E_r = exp\left(2.303 \times \frac{t}{a_e + b_e t}\right) \tag{6}$$

$$a_e = a_{e1} + a_{e2} * DS + a_{e3} * DS^2 \tag{7}$$

$$b_e = b_{e1} + b * DS \tag{8}$$

$$\left(f_c' - f_{c0}'\right) = \frac{(E_r - E_{r0})}{a_{er} + b_{er}(E_r - E_{r0})} \tag{9}$$

Table 5. Exponential function coefficients of the surface resistivity prediction model based on the DS content.

w/b	DS	Coefficients of Exponential Function		
		a_e	b_e	R^2
1.5	0	1.7948	1.1629	0.9173
	0.1	1.3136	1.1705	0.8551
	0.2	1.7087	1.2452	0.9403
	0.3	2.2119	1.4247	0.8837
	0.4	3.6567	1.4697	0.8670
	0.5	3.7226	1.5226	0.8825

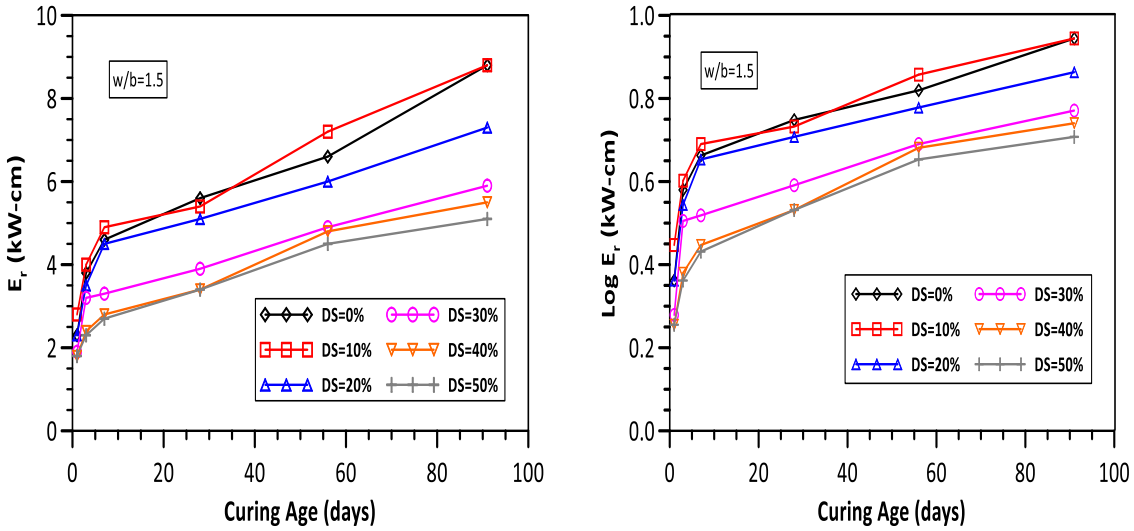

Figure 11. (**a**) The relationship between the curing age (t) and surface resistivity (E_r) of the CLSM (under normal scale coordinates). (**b**) The relationship between the curing age (t) and surface resistivity (E_r) of the CLSM (after transfer to semi-logarithm scale coordinates).

Under the same conditions, as a result of the test of resistivity, the coefficient a_e increases as the content of the DS increases. Therefore, a quadratic increment function between a_e and DS is used, which indicates that a_e has a relationship between a parabolic curve and a change in the content of the DS, as shown in Figure 12 and Equation (7). The coefficient b_e shows a linear relationship with the increase of the DS, as shown in Figure 13 and Equation (8).

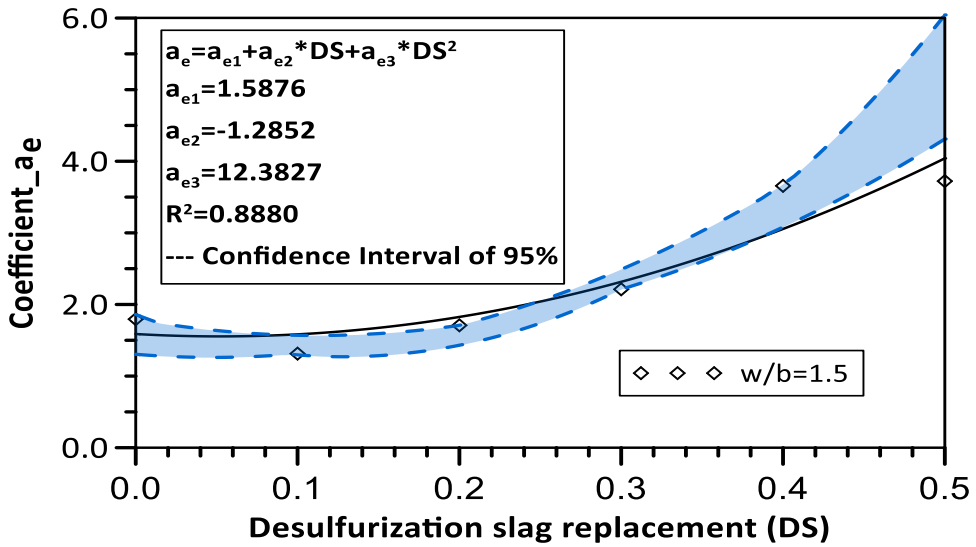

Figure 12. Characteristics of the coefficient a_e of the surface resistivity prediction model versus the DS content.

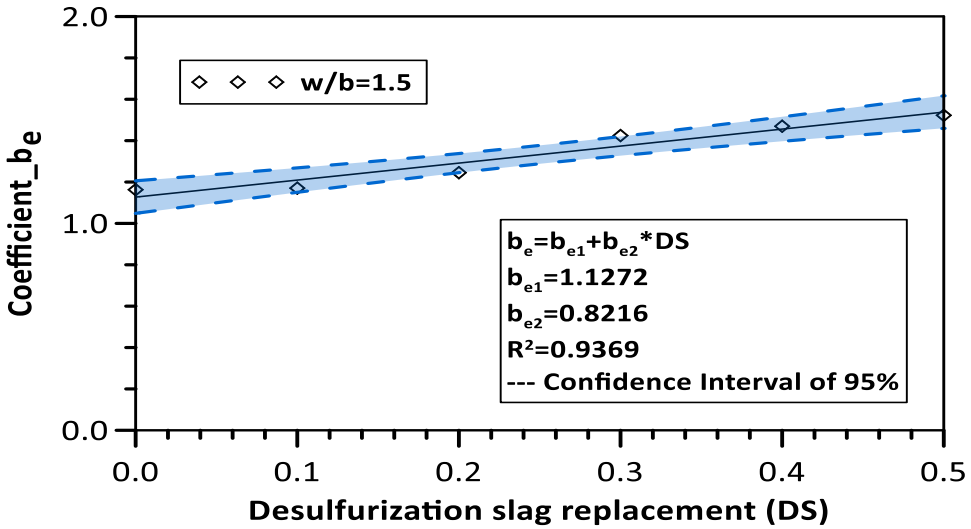

Figure 13. Characteristics of the coefficient b_e of the surface resistivity prediction model versus the DS content.

4.3. Relationship Between Compressive Strength and Electrical Resistivity

Previous researchers have applied the resistivity of concrete to predict the compressive strength, and such studies often involve the development of a relationship between resistivity and compressive strength. Previous studies have concluded that there is a good correlation between resistivity and compressive strength for concrete with a specific water-binder ratio. However, the compressive strength of concrete increases linearly or nonlinearly with resistivity (Lubeck et al., 2012 [19], Liu and Presuel-Moreno, 2014 [20], Xiaosheng et al., 2012 [21], Kahraman and Alber, 2014 [26], and Ramezanianpour et al., 2014 [27]). Thus, the relationship between the surface resistivity and compressive strength may be related to the water-binder ratio of the concrete. Figure 14 shows the test results between the surface resistivity and the compressive strength of the CLSM when the water-binder ratio is 1.5 and at different DS contents. For the same DS content, the compressive strength $f'_{c,}$ increases with the resistivity E_r, and the increasing trend is a smoothed nonlinear function. Thus, in the process of establishing the predictive model, the study will ignore the influence of the water-binder ratio's change and use the hyperbolic function to simulate the relationship between the compressive strength and resistivity of the CLSM, as shown in the Equation (9), Where a_{er} and b_{er} are hyperbolic function coefficients of the relationship prediction model between the compressive strength and electrical resistivity versus the DS contents and shown in Table 6. E_r is the surface resistivity of the CLSM, f'_{c0} is the initial compressive strength, and E_{r0} is the initial surface resistivity; f'_{c0} and E_{r0} will be directly obtained from the test results. Under the same conditions, based on the assumption of a fixed water-binder ratio, the coefficient a_{er} shows a tendency of the secondary parabola to rise first and then decrease as the content of the DS increases. The coefficient b_{er} decreases linearly with the increment of the replacement content of the DS, as shown in Table 6.

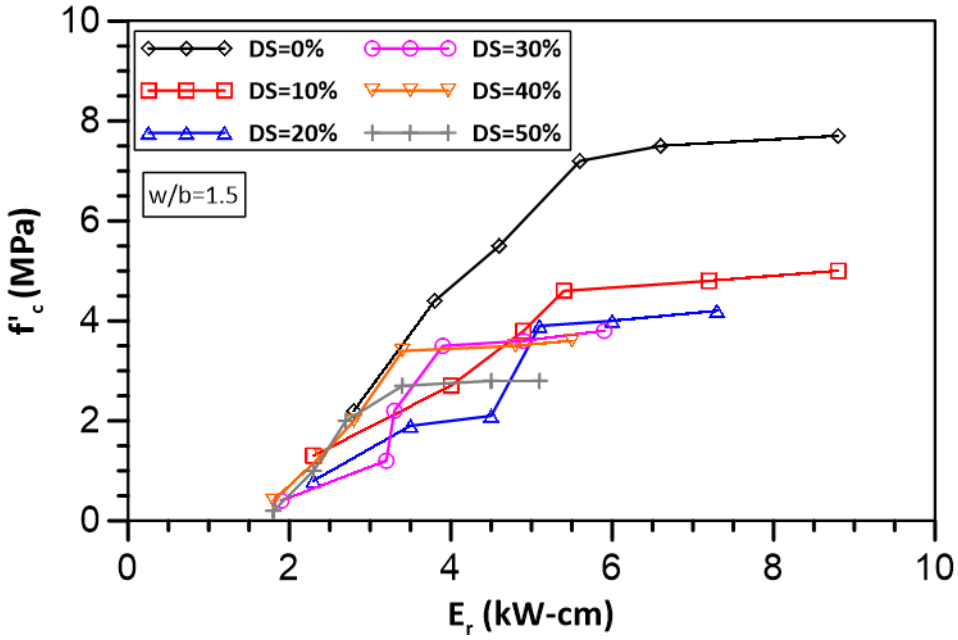

Figure 14. The relationship of the compressive strength and surface resistivity with various DS contents.

Table 6. Characteristics of the coefficients a_{er} and b_{er} of the relationship prediction model between the compressive strength and electrical resistivity versus the DS contents.

w/b	DS	Coefficients of Hyperbolic Function	
		a_{er}	b_{er}
1.5	0	0.4046	0.1070
	0.1	0.4516	0.1830
	0.2	0.8950	0.0955
	0.3	0.6342	0.1155
	0.4	0.3581	0.1994
	0.5	0.2990	0.2707

5. Comparison between Predictive Analysis and Test Results

5.1. Compressive Strength

Figure 15a,b shows the CLSM compressive strength analysis mode obtained by applying the compressive strength prediction analysis mode. Under the condition of the fixed water-binder ratio and different DS instead of a fine natural aggregate (the substitution amount is 0%, 10%, and 20% to 50%, respectively), the compressive strength and curing age of the CLSM are performed in a predictive analysis.

This study uses Equation (10) to discuss the mean absolute percentage error (MAPE) (Lewis [28]). When the MAPE value is less than 10%, it means it has excellent predictive ability. When the MAPE value is between 10% and 20%, it means a good predictive ability; when the MAPE value is introduced between 20% and 50%, it means that it has a reasonable predictive capability; when the MAPE value is greater than 50%, it means that the predictive ability is incorrect. Considering the compressive strength of the curing age of one day, the MAPE value of the prediction result of the total compressive strength of different DS replacement amounts is 13.88%, as shown in Figure 16a. However, if the strength of the one-day compressive test specimen is excluded, the predicted model and the measured MAPE values are 9.17%, as shown in Figure 16b. The main reason for the large variation in the prediction results is that the variability of the compressive test specimen strength at the one-day age is higher than that of the test samples at other ages. However, the overall analysis results show that the predicted

analytical values are quite close to the experimental results under the different DS replacements. Thus, the prediction model for the CLSM compressive strength proposed in this study can obtain good analytical results.

$$MAPE = \frac{1}{k}\sum_{i=1}^{k}\left|\frac{y_i - \hat{y_i}}{y_i}\right| \quad (10)$$

where y_i is a measurement, $\hat{y_i}$ is the mode analysis value, and k is the number of analysis data.

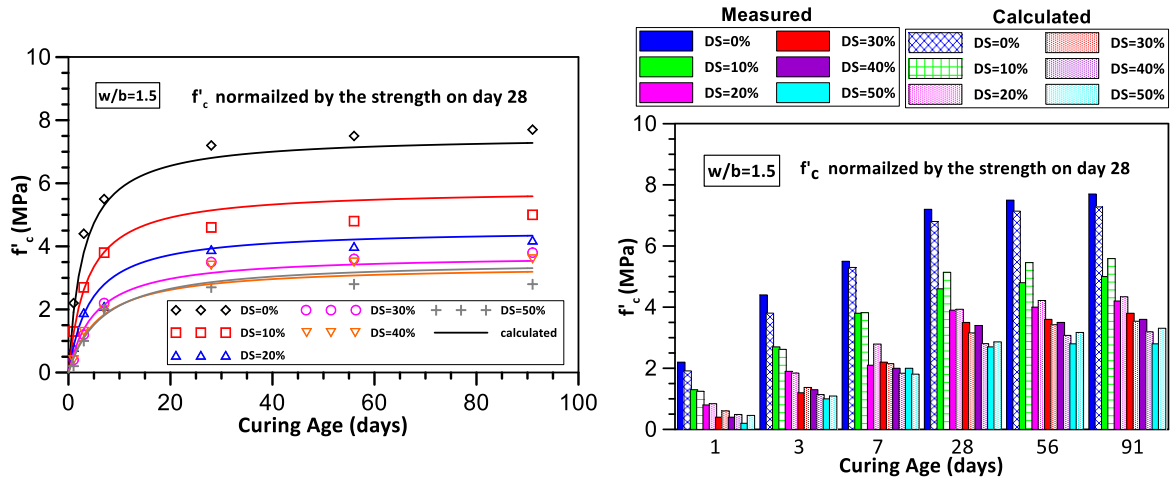

(**a**) (**b**)

Figure 15. (**a**) Comparison of the compressive strength between the predicted analysis and test results. (by curve graph) (**b**) Comparison of the compressive strength between the predicted analysis and test results. (by histogram)

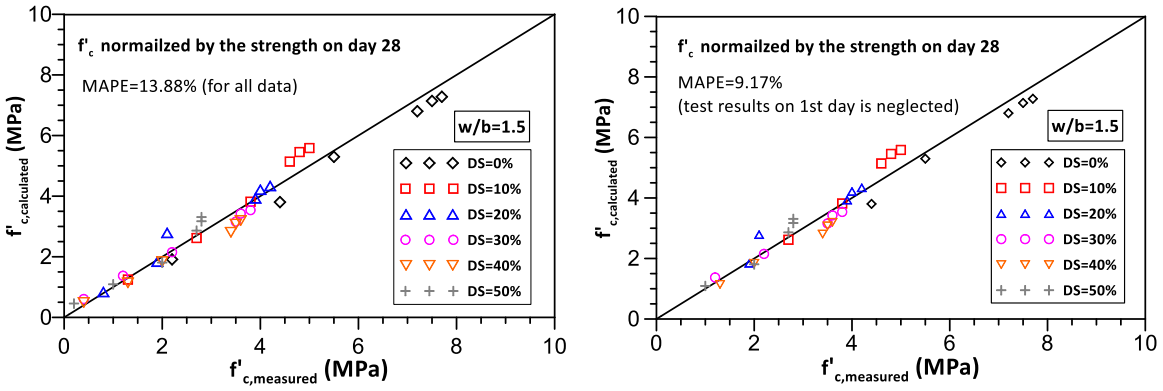

(**a**) (**b**)

Figure 16. (**a**) Mean absolute percentage error (MAPE) value by applying the compressive strength prediction analysis (considering the results obtained by all curing ages). (**b**) MAPE value by applying the compressive strength prediction analysis (excluding the results obtained from the 1-day sample).

5.2. Surface Resistivity

As shown in Figure 17a,b, under normal scale coordinates and semi-logarithmic scale coordinates and the exponential, the hyperbolic function model is used to predict the resistivity of the CLSM considering the curing age and fixed water-binder ratio. The trend of the different desulfurization slag contents was compared with the test results. The analysis results show that the resistivity prediction model based on the hyperbolic model is based on the relationship between the resistivity and curing age and can accurately evaluate the trend of resistivity change under different desulfurization slag contents and curing ages. The analysis shows that the MAPE value is 11.64% under different desulfurization slag contents and curing ages when the water-binder ratio is 1.5. Thus, the surface resistivity prediction model proposed by Wang (2017) [23] cannot accurately be simulated for the later resistivity increase trend, but the analysis result is also good. The MAPE value is only about 10%, as Lewis [28] proposed, but if the MAPE is less than 10%, the model has an excellent predictive capability. Thus, the surface resistivity prediction model set up in this study has a good predictive ability.

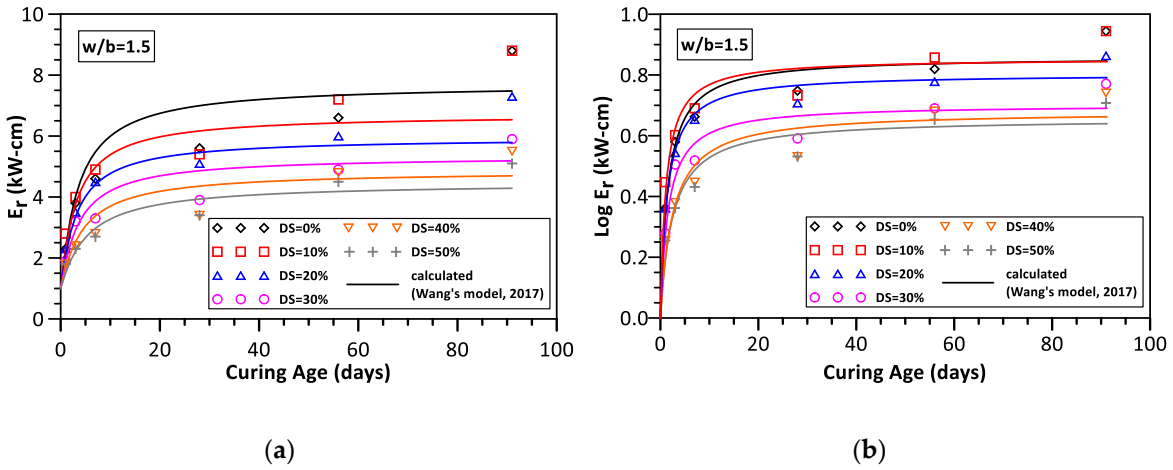

(**a**) (**b**)

Figure 17. (**a**) Comparison of the surface resistivity between the predicted analysis and test results (under normal scale coordinates). (**b**) Comparison of the surface resistivity between the predicted analysis and test results (after transfer to the semi-logarithm scale coordinates).

5.3. Relationship Between Compressive Strength and Surface Resistivity

In Figure 18a,b, when a CLSM is considered at a fixed water-binder ratio (w/b = 1.5), a hyperbolic function model is used to predict the relationship between the surface resistivity and compressive strength. As shown in Figure 18, the relationship between the surface resistivity and compressive strength of different curing times t and desulfurization slag contents was compared. The analysis results show the all determinate coefficients R^2 greater than 0.7, and the model based on the hyperbolic model to predict the compressive strength can accurately estimate the compressive strength under different desulfurization slag contents and curing ages t based on the resistivity data. This model is superior to the linear and logarithmic function regressions, and the trend is shown in Figure 18c,d. The analysis results show that, when the ratio of water to binder is 1.5, the MAPE value is 10.67%. Thus, predicting the compressive strength model of a CLSM by using the surface resistivity set up in this study has a good predictive ability.

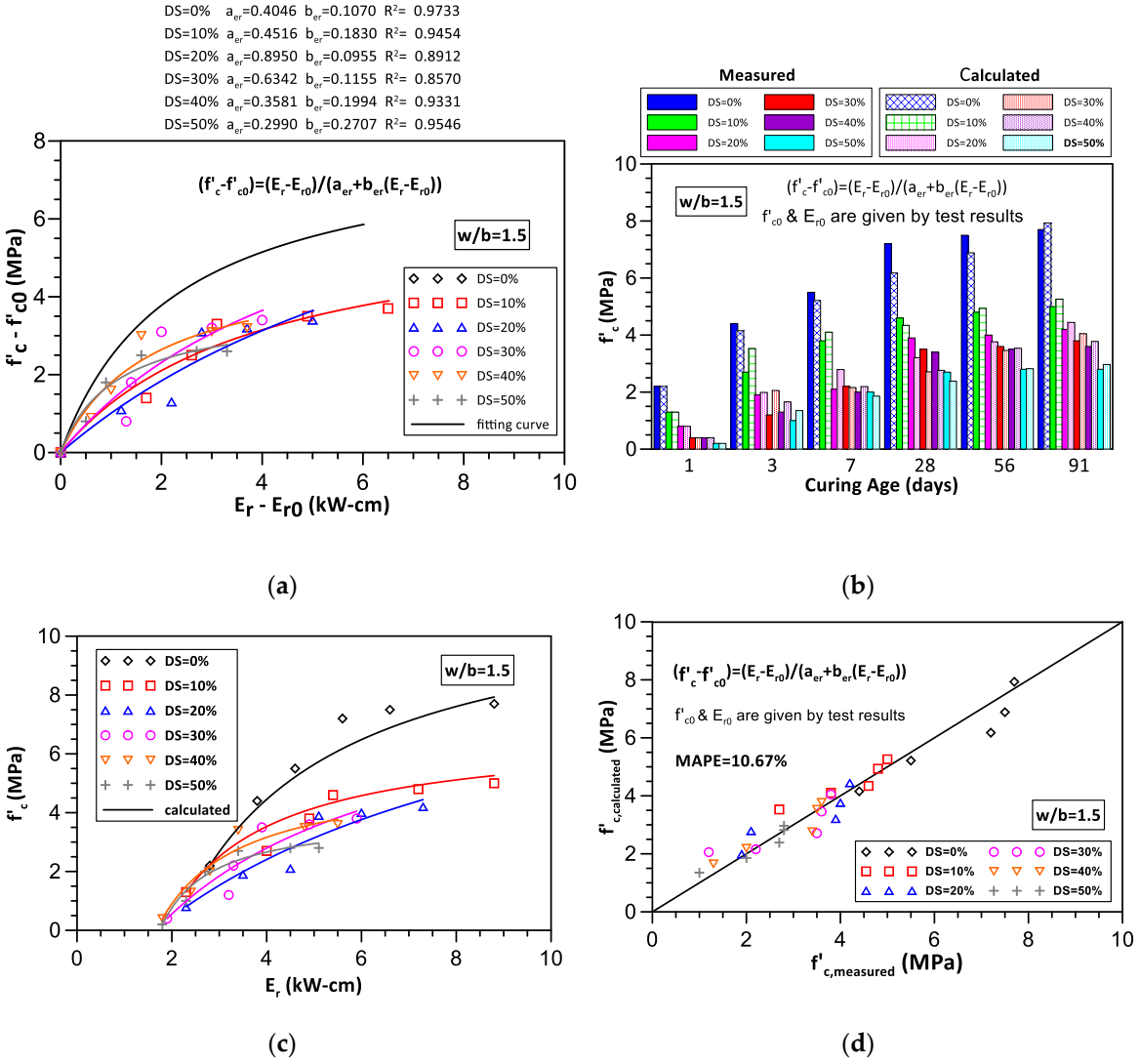

Figure 18. (**a**) Comparison of the predicted analysis and test results for the relationship between the compressive strength and surface resistivity (by curve graph). (**b**) Comparison of the predicted analysis and test results for the relationship between the compressive strength and surface resistivity (by histogram). (**c**) Comparison of the predicted analysis and test results for the relationship between the compressive strength and surface resistivity (hyperbolic function model). (**d**) MAPE value by applying the predicted analysis of the compressive strength and surface resistivity (hyperbolic function model).

6. Conclusions

This study mainly shows the influence trend of the compressive strength and resistivity of adding desulfurization slag to the CLSM and the optimal content of DS addition replacements and, according to relevant ASTM specifications, the fine aggregate of the CLSM material was replaced with desulfurization slag with a replacement proportion of 0~50% to test the compression strength and surface resistance of the CLSM under different curing times (1~120 days). After summarizing the test results, we tried to predict the trend of the compressive strength and surface resistivity based on a mathematical model to establish a good prediction model to provide a reference for future research and engineering applications. The research results are summarized as follows:

(1) The test results show that the compressive strength of the CLSM is inversely related to the replacement amounts of DS. When the replacement proportion of the DS increases but less than 20%, the compressive strength decreases rapidly with the increase of the replacement DS. When the replacement ratio of the DS is between 20% and 50%, the reduction in the compressive

strength value does not change much at any curing age. For the compressive strength on the 28th day, if the average amount of desulfurization slag replacement increases by 10%, the compressive strength is reduced by 0.9 MPa. Therefore, the 20% DS fine aggregate replacement proportion is a key recommended amount for the compressive strength of CLSMs.

(2) From the test results, the surface resistivity of the CLSM is inversely related to the replacement amount of the DS and directly proportional to the curing time. When the replacement proportion of the DS increases and exceeds 10%, the surface resistivity decreases rapidly with the increase of the replacement DS. When the replacement ratio of the DS is between 0% and 10%, the reduction in the surface resistivity value does not change much at any curing age. For the surface resistivity on the 28th day, if the average amount of desulfurization slag replacement increases by 10%, the surface resistivity is reduced by 0.9 kΩ-cm. Compared with the surface resistivity development of the previous 28-day value, it is most significant at the age of 28 to 56 days. The possible reason is that the hydration of the CLSM is completed in the late period, which increases the percentage of the resistivity value growth. Therefore, the 10% DS fine aggregate replacement proportion is a key recommended amount for the surface resistivity of CLSMs.

(3) Based on mathematical functions, this study explored the combined design of CLSMs and DS. We deduced, under a fixed water-binding rate (w/b = 1.5), various variables such as the change of the curing ages and the replacement proportions of fine aggregates by desulfurization slag, the prediction model of the compressive strength, and the surface resistivity of CLSMs. This provided future engineering design references for waste recycling and reuse.

(4) Inferring from the test results, the relationship between the different curing ages and replacement rates of the desulfurization slag and compressive strength is a hyperbolic function model, and the relationship with the surface resistivity is an exponential function. The relationship between the compressive strength and surface resistivity was analyzed through the prediction mode that is a nonlinear exponential function, which is very close to the experimental results. The above inference has been proven to be very close to the experimental results. These relationships cannot be obtained from general linear and nonlinear regression analyses.

(5) By comparing the compressive strength prediction model with the test results, it was found that the one-day compressive strength age was excluded, and the MAPE value was 9.17%. From the comparison between the prediction model of the surface resistivity with the test results, the MAPE of the prediction model of the surface resistivity was 11.64%. The prediction model value established by the relationship between the compressive strength and surface resistivity was compared with the test result, and the results showed that the MAPE value of the prediction model is 10.67%. Summarizing all the analysis results shows that the MAPE values of all the prediction models are about 10%, and the analysis model established in this study has a good prediction accuracy.

Author Contributions: H.-Y.W. conceived and designed the study. C.-C.H. and C.-C.W. performed the simulations. C.-C.H. and C.-C.W. wrote the main draft of the manuscript. C.-C.H. revised the manuscript. All authors contributed to the discussion of the results, and commented on the manuscript. All authors have read and agreed to the published version of the manuscript

Funding: This support of the Ministry of Science and Technology (MOST) under the Grant Most 109-2622-E-992-005-CC3 in Taiwan is gratefully acknowledged.

Conflicts of Interest: The authors declare no conflict of interest.

References

1. Kuo, W.T.; Weng, M.W. Utilization of desulfurization/granulated blast furnace slag as controlled low strength material without Portland cement. *J. Chung Cheng Inst. Technol.* **2009**, *38*, 157–166.
2. Cho, B.; Koo, K.-M.; Choi, S.-J. Compressive Strength and Microstructure Properties of Alkali-Activated Systems with Blast Furnace Slag, Desulfurization Slag, and Gypsum. *Adv. Civ. Eng.* **2018**, *2018*, 1–9. [CrossRef]
3. Zhang, W.; Choi, H.; Sagawa, T.; Hama, Y. Compressive strength development and durability of an environmental load-reduction material manufactured using circulating fluidized bed ash and blast-furnace slag. *Constr. Build. Mater.* **2017**, *146*, 102–113. [CrossRef]
4. Kuo, W.-T.; Shu, C.-Y. Application of high-temperature rapid catalytic technology to forecast the volumetric stability behavior of containing steel slag mixtures. *Constr. Build. Mater.* **2014**, *50*, 463–470. [CrossRef]
5. Kuo, W.-T. Properties of compressed concrete paving units made produced using desulfurization slag. *Environ. Prog. Sustain. Energy* **2015**, *34*, 1365–1371. [CrossRef]
6. Kuo, W.T.; Wang, H.Y.; Shu, C.Y. Engineering properties of cement less concrete produced from GGBFS and recycled desulfurization slag. *Constr. Build. Mater.* **2014**, *63*, 189–196. [CrossRef]
7. Zheng, Z. *Discussion on the Technical Capacity of Domestic Waste Recycling*; Industrial Technology Research Institute Environmental Safety Center: Hisnchu, Taiwan, 2003.
8. Xue, G.; Yilmaz, E.; Song, W.; Cao, S. Compressive Strength Characteristics of Cemented Tailings Backfill with Alkali-Activated Slag. *Appl. Sci.* **2018**, *8*, 1537. [CrossRef]
9. Lin, W.-T.; Weng, T.-L.; Cheng, A.; Chao, S.-J.; Hsu, H.-M. Properties of Controlled Low Strength Material with Circulating Fluidized Bed Combustion Ash and Recycled Aggregates. *Materials* **2018**, *11*, 715. [CrossRef]
10. Huang, L.-J.; Wang, H.-Y.; Wei, C.-T. Engineering properties of controlled low strength desulfurization slags (CLSDS). *Constr. Build. Mater.* **2016**, *115*, 6–12. [CrossRef]
11. ACI. *229R-94 Report: Controlled Low Strength Materials (CLSM), June (2013)*; Concrete International: Lamberton, CA, USA, 2013.
12. Zheng, R. Concrete Technology. *J. Taiwan Concr. Soc.* **2009**, *3*, 64–74.
13. Kaliyavaradhan, S.K.; Ling, T.-C.; Guo, M.-Z.; Mo, K.H. Waste resources recycling in controlled low-strength material (CLSM): A critical review on plastic properties. *J. Environ. Manag.* **2019**, *241*, 383–396. [CrossRef] [PubMed]
14. Wang, C.C. Prediction model of electrical resistivity and compressive strength of waste LCD glass concrete. *Comput. Concr.* **2017**, *19*, 467–475. [CrossRef]
15. Wang, C.C. Modelling of the compressive strength development of cement mortar with furnace slag and desulfurization slag from the early strength. *Constr. Build. Mater.* **2016**, *128*, 108–117. [CrossRef]
16. Kabir, A.; Hasan, M.; Miah, M.K. Predicting 28 days' compressive strength of concrete from 7 days' test result. In Proceedings of the International Conference on Advances in Design and Construction of Structures, Bangalore, India, 19–20 October 2012; pp. 18–22.
17. Kheder, G.F.; Gabban, A.M.A.; Abid, S.M. Mathematical model for the prediction of cement compressive strength at the ages of 7 and 28 days within 24 hours. *Mater. Struct.* **2003**, *36*, 693–701. [CrossRef]
18. Benaicha, M.; Burtschell, Y.; Alaoui, A.H. Prediction of compressive strength at early age of concrete —Application of maturity. *J. Build. Eng.* **2016**, *6*, 119–125. [CrossRef]
19. Lübeck, A.; Gastaldini, A.; Barin, D.; Siqueira, H. Compressive strength and electrical properties of concrete with white Portland cement and blast-furnace slag. *Cem. Concr. Compos.* **2012**, *34*, 392–399. [CrossRef]
20. Liu, Y.; Presuel-Moreno, F. Effect of elevated temperature curing on compressive strength and electrical resistivity of concrete with fly ash and ground-granulated blast-furnace slag. *ACI Mater. J.* **2014**, *111*, 531–541.
21. Wei, X.; Xiao, L.; Li, Z. Prediction of standard compressive strength of cement by the electrical resistivity measurement. *Constr. Build. Mater.* **2012**, *31*, 341–346. [CrossRef]
22. Ferreira, R.M.; Jalali, S. NDT measurements for the prediction of 28-day compressive strength. *NDT E Int.* **2010**, *43*, 55–61. [CrossRef]
23. Wang, C.C.; Wang, H.-Y.; Huang, C. Predictive models of hardened mechanical properties of waste LCD glass concrete. *Comput. Concr.* **2014**, *14*, 577–597. [CrossRef]
24. Alilou, V.K.; Teshnehlab, M. Prediction of 28-day compressive strength of concrete on the third day using artificial neural networks. *Internatl. J. Eng.* **2010**, *3*, 565–576.

25. Wang, H.-Y.; Chen, J.-S. Mix proportions and properties of CLSC made from thin film transition liquid crystal display optical waste glass. *J. Environ. Manag.* **2010**, *91*, 638–645. [CrossRef] [PubMed]
26. Kahraman, S.; Alber, M. Electrical impedance spectroscopy measurements to estimate the uniaxial compressive strength of a fault breccia. *Bull. Mater. Sci.* **2014**, *37*, 1543–1550. [CrossRef]
27. Ramezanianpour, A.; Karein, S.M.M.; Vosoughi, P.; Pilvar, A.; Isapour, S.; Moodi, F. Effects of calcined perlite powder as a SCM on the strength and permeability of concrete. *Constr. Build. Mater.* **2014**, *66*, 222–228. [CrossRef]
28. Lewis, C.D. *Industrial and Business Forecasting Methods: A Practical Guide to Exponential Smoothing and Curve Fitting, London*; Butterworth Scientific Publishers: London, UK, 1982.